Environmental Science Processes & Impacts

ROYAL SOCIETY OF CHEMISTRY

PAPER

View Article Online
View Journal | View Issue

Cite this: *Environ. Sci.: Processes Impacts*, 2025, **27**, 2968

Rainfall-induced lateral and vertical microplastic transport of varying sizes in agricultural fields

Emilee Severe, †*[a] Saunak Sinha Ray, †[b] Wang Li,[c] David Zumr,[b] Tomáš Dostál,[b] Ben W. J. Surridge,[a] Josef Krasa,[b] Florian Wilken,[d] Peter Fiener,[d] Christine Stumpp,[c] Ahsan Maqbool,[e] José Alfonso Gómez,[e] Christian Zafiu[f] and John Quinton[a]

Agricultural soils, particularly those utilizing plastic products for crop production, are increasingly recognized as sources of microplastics (MPs) to aquatic ecosystems. In this research, we investigate the transport of polyethylene MPs of three different size ranges (53–63 μm, 125–150 μm and 425–500 μm) in an agricultural soil during a plot-based rainfall simulation. Using a combination of fluorescent particles and high-frequency photography, we tracked the number of MPs on the soil surface throughout the rainfall simulation, measured the depth MPs migrated into the soil profile and the number of MPs which were transported in surface runoff. Our results show that MPs had dynamic movement on the soil surface throughout the rainfall simulation. Approximately 20% of MPs sized 125–150 μm and 425–500 μm were exported from the plot in surface runoff with the remaining 80% of MPs thought to be retained in the soil. No significant differences were found in the number of MPs transported in surface runoff between MPs sized 125–150 μm and 425–500 μm. Microplastics were found to be enriched in eroded sediments. Microplastics of all sizes 53–63 μm, 125–150 μm and 425–500 μm were found in soil as deep as 8 cm with the majority of MPs found in the 0–2 cm soil depth. Results from this research not only indicate that MPs are quite mobile both vertically and laterally during rainfall events but also show that soils effectively retain and accumulate a sizeable proportion of MPs during heavy rainfall events.

Received 21st April 2025
Accepted 13th August 2025

DOI: 10.1039/d5em00304k

rsc.li/espi

Environmental significance

The transport of microplastics (MPs) from agricultural soils is increasingly recognized as a significant source of MPs to aquatic ecosystems through erosion processes. This study provides field-based evidence of lateral and vertical transport of MPs during rainfall events, demonstrating that soils can simultaneously act as sources and sinks of MPs. Our findings reveal that MPs are highly mobile, both vertically in the soil and laterally in surface runoff. These insights are critical for understanding MP fate in terrestrial systems, MP accumulation in aquatic ecosystems, and informing future land management practices aimed at mitigating plastic pollution from agricultural landscapes.

1. Introduction

Microplastics (MPs), currently defined as pieces of plastic between 1 μm and 5 mm in size, have been frequently detected in freshwater ecosystems across the globe.[1–3] The presence and accumulation of MPs in these environments raise concern due to their demonstrated negative impacts on aquatic organisms.[4–6] Amongst the various pathways by which MPs enter freshwater ecosystems, soils are increasingly recognized as a significant source.[7–11]

Agricultural activities represent a key contributor to soil MP contamination. In 2019 alone, approximately 708 kt of plastic were used for agricultural production in the EU,[12] with polyethylene (PE) being the most common polymer type. Agricultural plastic products, such as polytunnels, mulching films, polymer coated fertilizers, and irrigation tape, are used to increase crop production while simultaneously decreasing pesticide, irrigation, and fertilizer inputs.[13,14] Over time, these materials degrade and fragment, through various means into macro-, micro- and nano- sized plastic pieces which persist in soils and are challenging to remove.[15,16] Additionally, agricultural soils may be contaminated with MPs through secondary

[a]*Lancaster Environment Centre, Lancaster University, Lancaster, UK. E-mail: e.severe@lancaster.ac.uk; j.quinton@lancaster.ac.uk*

[b]*Faculty of Civil Engineering, Czech Technical University in Prague, Thakurova 7, 16629 Prague, Czech Republic*

[c]*Department of Water, Atmosphere and Environment, Institute of Soil Physics and Rural Water Management, University of Natural Resources and Life Sciences, Vienna, Muthgasse 18, 1190 Vienna, Austria*

[d]*Institute of Geography, University of Augsburg, Alter Postweg 118, 86159 Augsburg, Germany*

[e]*Institute for Sustainable Agriculture, CSIC, Cordoba 14004, Spain*

[f]*Department of Water, Atmosphere and Environment, Institute of Waste Management and Circular Economy, University of Natural Resources and Life Sciences, Vienna, Muthgasse 18, 1190 Vienna, Austria*

† Shared first authorship.

sources, such as the application of sewage sludge,[17,18] compost,[19–21] tire wear particles from nearby roads,[22] litter[19] and atmospheric deposition.[23]

Driven by the multitude of input sources and very long half-lives of most conventional plastics,[24] MPs accumulate in soils. Rainfall-induced erosion processes such as surface runoff may lead to the export of MPs to these water bodies.[9] Alternatively, infiltrating water from rainfall could facilitate the retention of MPs in soils by transporting them vertically within the soil profile.[25] The transport pathways—whether MPs move laterally with surface runoff or vertically into the soil profile, are influenced by a combination of soil physical properties (*e.g.*, porosity, erodibility)[26] and the physical characteristics of the MPs themselves.[8] Among these, MP size likely plays a critical role in determining the transport pathway and ultimate fate of MPs during erosion events.[8,27]

However, current understanding of MP size-dependent transport pathways and the rates of MP transport is limited as most research is laboratory based, uses limited MP size ranges, and investigates either MP transport in surface runoff or infiltration into the soil profile but not both potential transport pathways in tandem. It is widely thought that as size decreases, MPs are more mobile in soil and reach deeper soil layers than relatively larger MPs. This is especially shown in laboratory based column experiments where physical straining has been found to be a dominate process limiting the transport of large MPs compared to small MPs in their research.[28–31] Though findings from Du *et al.*[25] showed size-dependent transport to be nuanced as they found MP sized 25–147 μm had the highest vertical migration ability followed by MPs sized 0–25 μm then 147–250 μm. Maqbool *et al.*[26] found a similar pattern in soils with macropores, MPs sized 75–90 μm and 125–150 μm were leached through the soil column at higher rates than MPs sized 53–63 μm. Likewise under field conditions, some studies report no patterns of size-dependent migration,[32,33] while Rehm *et al.*[8] found MPs sized 53–100 μm migrated deeper in the soil compared to MP sized 250–300 μm, over the period of 1.5 years as affected by infiltrating water and the activity of soil organisms.[8] These results suggest that processes such as MP-colloid heteroaggregation[8,34,35] or interactions with the soil pore surface[26,35] could hinder small MP vertical transport through soil pores, a pattern which has been observed for other soil particles.[36]

Compared to vertical transport, fewer studies have investigated size dependent MP transport in surface runoff. One study found that as MP size decreases a greater number of particles were transported, specifically, MPs <50 μm were transported in higher numbers than MPs sized 50–100 μm, 100–200 μm and 200–500 μm.[37] Other research investigating the effect of size on MP transport in surface runoff has found, generally, MPs >1000 μm and <250 μm show less mobility than MPs sized 250–1000 μm.[8,27,38] In surface runoff, larger MPs require greater shear forces to become mobilized,[39] however smaller MPs are prone to bind with other soil particles[8] together, these processes may reduce MP transport as a function of size.

The aim of this research was to simultaneously quantify the relative roles between lateral and vertical MP redistribution during simulated rainfall events in field conditions. To determine how MP size affects the transport pathways followed during a rainfall simulation, three size ranges (53–63 μm, 125–150 μm, and 425–500 μm) of fluorescent MPs were used. We hypothesized that: (i) MPs of each size range will show a primary transport pathway, with a greater number of the largest MP size (425–500 μm) being transported in surface runoff due to less interaction with soil particles and limited vertical transport as compared to the smaller MP sizes (125–150 μm and 53–63 μm); and (ii) MPs sized 125–150 μm will infiltrate to the greatest depth in the soil profile, because vertical transport of the 425–500 μm MPs will be hindered due to small pore sizes within the soil matrix, and the 53–63 μm MPs will adhere to surrounding soil particles and therefore be retained in the top layers of soil. This research is critical for understanding the retention and mobilization of MPs in soil as well as characterizing MP size-dependent transport pathways during heavy rainfall events.

2. Methods

2.1 Site description and experimental set-up

Rainfall simulations took place on a farm near Řisuty which is approximately 30 km northwest of Prague in the Czech Republic (50°13′2.0″N, 14°1′2.2″E). The topsoil is classified as a Cambisol with a loam texture, consisting of 18.3% clay, 33.8% silt, and 47.9% sand and an organic carbon content ranging from 1.2% to 1.5%. More information about the field site and soil can be found in Jeřábek *et al.*,[40] Li *et al.*,[41] and Stašek *et al.*[42] Five experimental plots (1 m × 1 m) were prepared on a uniformly north-oriented 9° slope. Vegetation was manually removed from the fallow soil, and the soil was tilled using a rototiller to a depth of 10 cm.

Fluorescent polyethylene (PE) microspheres (Cospheric LLC) of three differing size ranges and colors 425–500 μm (red), 125–150 μm (green) and 53–63 μm (yellow) were used (SI Fig. S1). The 125–150 μm and 53–63 μm MPs had densities of 1.00 g cm^{-3} while the 425–500 μm MP had a slightly higher density of 1.09 g cm^{-3}. Fluorescent particles were chosen for convenient sample analysis and to track the movement of the MPs over the soil surface using a novel, high frequency photographic approach throughout the rainfall simulation.

A homogeneous mixture of soil and MP particles was created by adding 1.35×10^5 MP particles sized 53–63 μm and 125–150 μm and 1.24×10^5 of MP sized 425–500 μm into 12.5 kg of topsoil sieved to 15 mm. Soil was collected to a depth of approximately 15 cm and MPs were mixed at its ambient moisture content (~14% volumetric water content) on the night of the simulations. In total, 3.94×10^5 MPs were mixed into the soil, creating a 0.058% w/w mixture. The MP-soil mixture was applied evenly to the plot to create a 1 cm topsoil layer. Once the MP-soil mixture had been applied to the plots, the topsoil was compacted to ensure uniform initial conditions across all plots, using a 50 kg rolling press applying a pressure of approximately 20 kPa, resulting in a bulk density of 1.24 g cm^{-3} and a porosity of 0.48 ± 0.03.

Soil moisture in the topsoil (<15 cm) was measured before the rainfall simulation and 15 min after the wet run (see below),

using a soil moisture probe (HydroSense II HS2, Campbell Scientific) at six locations within each plot.

Rainfall was applied with a pressure-fed swinging nozzle rainfall simulator at a rainfall intensity of 60 mm h^{-1} (Fig. 1). High rainfall rates such as this are frequently used in erosion experiments,[8,42,43] as they simulate short-duration, high intensity storms increasing observed under extreme weather conditions in Central Europe.[44,45] The simulator produces raindrops with a kinetic energy of 4.14 J m^{-2} mm^{-1} and Christiansen's uniformity coefficient of 93%.[46] A simulation procedure similar to Neumann *et al.*[47] and Stašek *et al.*[42] was followed. Rainfall simulation on each plot comprised of three phases: (i) a "dry run" simulation executed at "dry" ambient soil moisture lasting 30 min after surface runoff commenced; (ii) a 15-min interval where the simulator was turned off to facilitate infiltration and sediment deposition; (iii) a second "wet run" simulation on the wet soil for 30 min after surface runoff commenced at the same settings. The time of rainfall initiation and subsequent surface runoff commencement were recorded. The commencement of surface runoff was determined visually when a steady flow of water was delivered from the plots.

Deuterated water was utilized as a conservative tracer to trace the extent to which simulated rainwater infiltrated into the soil profile. Exactly, 50 mL Deuterium oxide (99.96 atom % D, Sigma-Aldrich) was added to a 1000 L water reservoir (δ^2H, $-64.20 \pm 0.56‰$) which was used to supply water for the rainfall simulations. Rainwater samples were taken during the experiment for each plot, and the δ^2H ratio was measured for identical tracer input across each plot. Furthermore, soil near the plots were sampled before experiments, to get the background soil water δ^2H signature.

2.2 Observations during the simulation and sample collection

Methods employed by Severe *et al.*[48] were used to track the number of MPs on the soil surface throughout the rainfall simulation. To observe the MP particle movement during the rainfall simulations, the entire 1 m × 1 m surface of the plot was imaged throughout the rainfall simulation using UV photography methods. Images of the soil surface were captured every ~10 s during each simulation using a Canon EOS 850D camera. An 18–55 mm zoom lens set at a focal length of 26 mm was used with the following camera settings: *f*/7.1, exposure 1 s and ISO 320. For each plot, the camera was set 78 cm from the bottom boundary of the plot, at a height of 165 cm. Simulations were performed overnight, in the absence of natural light, and plots were illuminated by a 365 nm wide beam UV 50-watt flood lamp (Mark SG Enterprises). Due to technical difficulties with the UV lamp during the rainfall simulation on the first plot, results from that plot were omitted from analysis of surface movement of MPs.

During both the dry and wet runs, surface runoff leaving the bottom edge of the plots was subsampled in glass bottles with tin caps every 2.5 min for a total of 30 minutes. Collection time of surface runoff was recorded for each sample. Runoff samples were collected from all 5 plots.

A stainless-steel column (length: 13 cm; inner diameter: 6.5 cm) with openings on two sides at every 2 cm was used to collect soil samples. Soil samples were collected from plots number 1 and 2 and the other plots were left intact to study the long-term MP transport. To obtain a representative MP retention profile per plot, composite soil sampling was used and samples were taken from 5 different locations (one sample on each corner, and one sample in the middle of the 1 m × 1 m plot). The soil plasticity was too high for depth explicit soil sampling directly

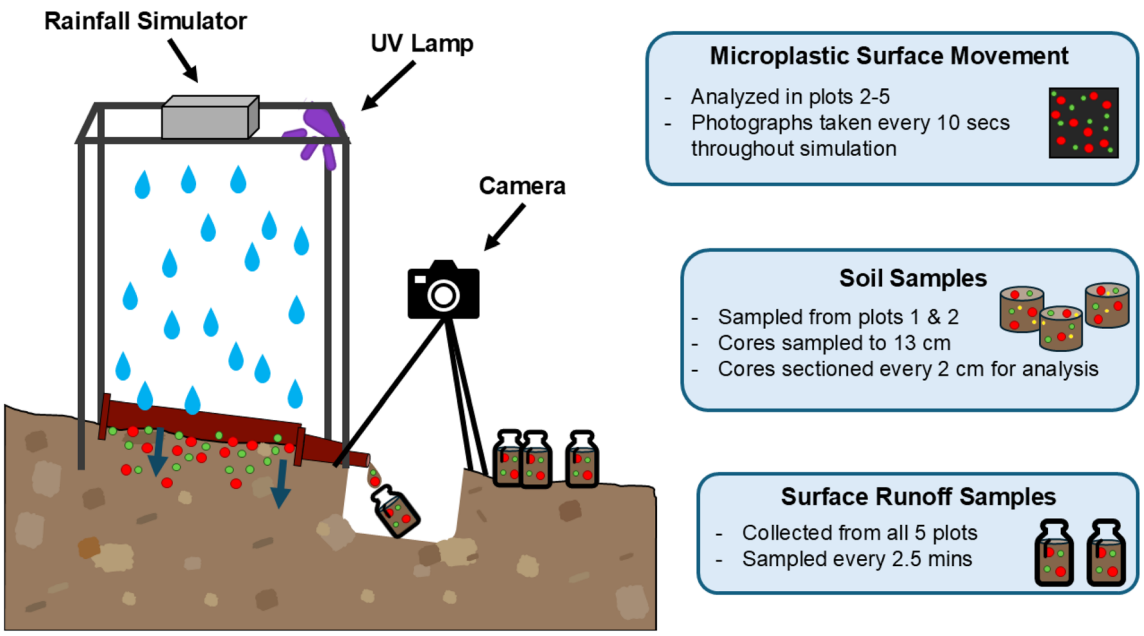

Fig. 1 Diagram showing the experimental set-up and sample collection.

after rainfall simulation, therefore, soil samples were taken after 5 hours after the end of the wet run simulation. Soil water isotopic signature and MPs were analysed within the following depth increments: 0–2 cm, 2–4 cm, 4–6 cm, 6–8 cm, 8–11 cm, and 11–13 cm to reveal the water flow and MP retention profile.

2.3 Sample analysis and microplastic extraction

2.3.1 Microplastic soil surface movement image processing and analysis. Images were captured in RAW format and converted to TIFF format (LZW compression) using Adobe Photoshop (version 26.3). Due to the position of the rainfall simulator, the camera could not be located orthogonally in relation to the plots. Therefore, a single pixel in the foreground of the images (or front of the plot) represented a larger spatial area than the pixels in the background (or rear of the plot). The Perspective Warp tool (stretch function) in Adobe Photoshop was used to resample the images, correcting the perspective in the images.[49] Photogrammetry targets were placed outside of the plots to validate the resampling.[50]

Each image was cropped to a 3400 × 3400-pixel area in Image J (version 1.54f) which is equivalent to 0.98 m × 0.98 m area, giving a ~1 cm buffer from the borders of the plot. These 1 cm buffer areas were created to remove MPs stuck to the borders of the plot from the image and remove the potential edge effects of the border on MP retention or removal.[51]

To enhance the visibility of the particle colors, the maximum brightness intensity for each image was adjusted. This type of image adjustment is widely accepted as long as care is taken to not over-saturate the brightness intensity and thus lose data in the images.[52] As our images were very dark (on a scale of 0–255, mean brightness intensity ~8.6), such adjustment was warranted. As the brightness intensity of each image varied slightly, the average value needed to readjust the maximum brightness value was calculated and the maximum brightness value was adjusted to 135 in Image J.

Images were then processed through the Color Thresholding tool in Image J to quantify the number of MPs in each image, using a HSB color space specific to each particle size. The, yellow, 53–63 μm particle size range was not considered in our analysis of the MP surface movement as it could not be detected by the digital camera. The following thresholds were set for each of the following MPs: 425–500 μm (red) MPs: hue = 45–220 ("pass" or band-reject), saturation = 55–255, brightness = 85–255; 125–150 μm (green) MPs: hue = 45–95, saturation = 45–255, brightness = 45–255. The watershed separation tool was then used to detect and separate potential adjoining particles (Fig. 2).

The dynamic nature of the soil surface (*i.e.* variable surface microtopography, surface flows of water) during the rainfall simulation made it difficult to quantify the effectiveness of MP detection. However, a small validation plot was prepared in an identical manner to the other plots described above, with a known number of MP particles spread on the surface of the plot and photographed. No rainfall was applied to this validation plot. Of the 60 MPs sized 425–500 μm and 441 MPs sized 125–150 μm which were spread on the surface of the validation plot, 51 (85%) of the 425–500 μm and 132 (30%) of the 125–150 μm were visible in the images. Due to the porous nature of the soil and due to surface topography, it is likely that the particles which were not detected in the validation plots, migrated into the soil profile or were hidden from view of the camera after being spread on the soil surface.

To determine the effectiveness of correctly identifying MPs detected in the images; subsections of the images from the main 1 m × 1 m plots before, during and after the rainfall simulations were manually counted and considered as ground truth data in this study. Performance was assessed by calculating the *f*-score for each particle size. The *f*-score considers both the proportion of particles detected and the proportion of the detected particles which were correctly labelled in the thresholding procedure. *F*-Score is calculated on a scale of 0–1, where 1 indicates the best performance. The 425–500 μm MP had an *f*-score of 0.94 and the 125–150 μm MP had an *f*-score of 0.82 meaning that 94% and 82% of 425–500 μm MPs and 125–150 μm MPs respectively, which were visible in the images, were correctly classified.

2.3.2 Surface runoff and sediment analysis. After collection, bottled runoff samples were weighed then dried in an oven at 60 °C for 24–32 hours, then re-weighed to determine the mass of sediment and the volume of runoff delivered from the plots. The method described in Sinha Ray *et al.*[53] was used to analyse MPs in surface runoff sediments. In summary, 100 mL of distilled water was added to the dried sediments in the bottles, followed by ultrasonication (40 kHz) and overhead stirring (500 rpm) for 5 min each to dislodge settled sediments and release entrapped MPs. Samples were wet sieved (1 mm, 500 μm, 425 μm, 150 μm and 125 μm) to separate the fluorescent MPs and sediments by sizes. Sampling bottles were decanted and sieved using distilled water over a period of 5 min. The material remaining on the 425 μm and 125 μm sieves was filtered onto separate filter papers (pore size 0.7 μm) and oven-dried at 40 °C.

Samples from the filter paper were spread as a thin layer onto an opaque black tray (30 cm × 45 cm). A portable darkroom (Ilford Photo), using a 365 nm wide beam UV 50-watt flood lamp (Mark SG Enterprises) angled at 45° and a digital camera (Sony Alpha model α6000), placed at a vertical distance of 55 cm above the sampling tray were used to capture darkroom images of the prepared samples. Camera settings were fixed at: *f*/5.6, exposure 0.2 s, and ISO 100.

The color thresholding tool in Image J was used to detect the number of each MP size in the plots using the HSB color space. The following thresholds were set for each of the following MPs: 425–500 μm (red) MPs: hue = 0–45, saturation = 0–255, brightness = 130–255; 125–150 μm (green) MPs: hue = 50–145, saturation = 0–255, brightness = 130–255. Following the thresholding, a watershed separation was used to detect and separate adjacent particles, which may have been erroneously counted as one MP. A shape threshold was then applied to select particles with a circularity of 0.95–1.0, with 1.0 being a perfect circular shape. To count the number of MPs which were clustered together in the images, the area of each MP particle was divided by the median area of the MP (specific for

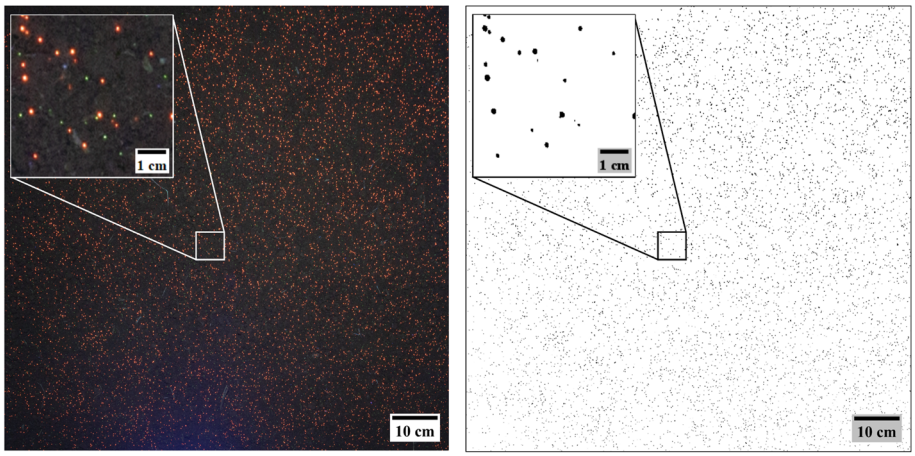

Fig. 2 Images demonstrating the particle detection from the images of the soil surface. Image of the soil surface after perspective correction and cropping (left). Thresholded image detecting the 425–500 μm (red) MPs, black dots are detected MPs (right).

each size range) in order to estimate the number of individual MPs within clusters.

Validation of this method is described in Sinha Ray *et al.*[53] The mean recovery rates were 84.9 ± 3.6% ($n = 15$) for the 125–150 μm MPs and 91.2 ± 2.8% ($n = 15$) for the 425–500 μm MPs. The 425–500 μm MP had an *f*-score of 0.93 and the 125–150 μm MP had an *f*-score of 0.89 meaning that 93% and 89% of 425–500 μm MPs and 125–150 μm MPs respectively, which were visible in the images, were correctly classified.

2.3.3 Soil microplastic analysis and isotope analysis. As the density of MPs applied in this experiment was less than 1.1 g cm^{-3}, saturated NaCl (1.2 g cm^{-3}) was selected for density separation to extract MPs from collected soil samples, which is cost-effective and non-toxic. The complete soil mass in each sample, ranging from 130–650 g depending on soil sample depth, was analysed. Collected soil samples were placed in 1000 mL beakers, with 400 mL saturated NaCl and 2 mL H_2O_2 (30%) added. A glass stirring rod was used to mix the soil sample and the added solution. The supernatant was then collected into a 500 mL beaker after overnight settlement.[54] The entire process was repeated 3 times to maximize the extraction efficiency. A UV lamp was used to identify residual MPs and ensure that no MPs were left on glassware. Considering the wide particle size range (53 μm to 500 μm), the collected supernatant was then further separated into different fractions by using sieves with openings of 53 μm, and 500 μm. Afterward, collected MPs were filtered through a vacuum filtration system using regenerated cellulose filters (47 mm diameter, 8 μm pore size). All filters were then imaged with a confocal laser scanning microscope (SP8, Leica). The entire filter was analysed with an exposure time of 1.00 ms, gain 1.0, and camera magnification of 5×, which provided a good image and reasonable scanning time for the entire filter. As the peak excitation and emission wavelengths varied for each MP, different fluorescent filter cubes where used. For the red (425–500 μm) MP the fluorescent filter cube RHOD (excitation 541–551 and emission 565–605) was used and the GFP filter cube (excitation 450–490 and emission 500–550) was used for the yellow (53–63 μm) MPs and green (125–150 μm) MPs.

Rainfall water and soil samples pore water were analysed for δ^2H with a Cavity Ring-Down Isotope Spectrophotometer Spectroscopy (Picarro L2130-i) with a precision of ±1‰. The water-vapor equilibration method was employed to test the soil water isotopic signature.[55,56] Briefly, soil samples were collected in double resealable zipper bags with air pushed out and stored in the fridge (4 °C) before measurement to avoid soil moisture loss due to evaporation. To ensure water-vapor equilibrium in the headspace, collected soil sample bags were inflated with dry synthetic air and left for 3 days at laboratory conditions (20–22 °C). After that, the bag was punctured with a needle that connected to the Picarro L2130-i laser analyser which was used to quantify isotope levels.[55]

2.4 Data analysis

To understand the relationship between soil and MP transport, an enrichment ratio (ER) was calculated using eqn (1) wherein ER is the Enrichment Ratio, C_s is the MP concentration in the eroded sediments (number of MPs per g of sediment transported in surface runoff), and C_o is the MP concentration in the topsoil (number of MPs per g of topsoil).

$$ER = \frac{C_s}{C_o} \quad (1)$$

Enrichment ratio (ER) calculated by dividing the microplastic concentration in the sediments (C_S) by the microplastic concentration in the topsoil (C_O)

A value >1 indicates an enrichment of MPs in sediments transported in surface runoff and a value <1 indicates a reduction in the concentration of the MPs transported in sediments compared to the concentration of MPs in the topsoil.

Runoff coefficients were calculated for each rainfall simulation in order to understand the proportion of rainwater which infiltrated into the soil and was transported in surface runoff. The coefficient is calculated by dividing the volume of runoff by the total volume of rainfall applied to the plot. A coefficient of

0 indicates that all rainwater was held in the soil and a coefficient of 1 indicates that all rainwater became surface runoff.

All results are reported as mean ± standard deviation unless otherwise noted. Statistical analysis was conducted using R Statistical Software version 4.3.1.[57] Data normality and homogeneity were tested visually by inspecting histograms and using Kolmogorov–Smirnov and D'Agostino-Pearson's K^2 test to a 0.05 significance. When data were normally distributed Welch's *t*-tests were carried out to check for significant differences between treatments. When data were not normally distributed, Kruskal–Wallis tests were used along with Wilcoxen rank sum post-hoc tests to determine significant differences between treatments. Changepoint analysis of the mean and variance to detect a possible change in trend, was used to identify time points where the mean rate of change and variance changed significantly for particles detected on the soil surface. Changepoints were calculated using the PELT method in the R changepoint package.[58] As changepoint analysis requires data with regular interval, the number of MPs for each time point were averaged between plots and used in the analysis.

3. Results

3.1 Microplastic delivery in surface runoff

Across all plots, no substantial variation was detected in the initial soil moisture conditions prior to the dry run rainfall simulations, with the mean volumetric water content (VWC) being 14.0 ± 1.3%. The time it took for surface runoff commencement in each plot varied slightly. In the dry runs surface runoff commencement ranged from 3 to 6 min after the start of rainfall with a mean start time of 4 min and 13 s ± 55 s. In the wet runs, surface runoff commencement had a mean start time of 44s ± 18 s. The mean topsoil VWC for the wet run simulations was 25.8 ± 3.2%. During the rainfall simulations, runoff coefficients of 0.29 ± 0.01 ($n = 5$) and 0.37 ± 0.02 ($n = 5$) were produced for dry and wet runs, respectively. Similar runoff volumes and little variability in runoff rates were observed across all five replicate plots (Fig. 3). Overall, the mean runoff rates for wet runs (0.94 ± 0.12 L min^{-1}) were statistically higher than those for dry runs (0.74 ± 0.17 L min^{-1}) (t (111.02) = −7.29, $p < 0.001$). In general, the dry and wet runs sediment delivery rates followed the surface runoff dynamics (Fig. 3), wherein an initial flux of sediment movement was observed at the start of runoff, and sediment delivery peaked around the same time as peak runoff. A higher mean sediment delivery was observed in the wet runs 8.3 ± 0.95 g L^{-1} than in the dry runs 9.15 ± 1.53 g L^{-1} (t (93.11) = 3.56, $p = 0.0006$).

In case of the dry runs, the number of MPs transported from the plots in surface runoff peaked in the first 10 min and then declined as the rainfall simulation progressed. This pattern was only shown for one plot in case of the wet runs (Fig. 4). During the dry run simulation, 861 ± 358 MP L^{-1} and 854 ± 411 MP L^{-1} of the MPs sized 125–150 μm and 425–500 μm, respectively, were transported from the plots in surface runoff (Fig. 4). The wet runs had lower concentrations of MPs transported from the plots in surface runoff at 280 ± 160 MP L^{-1} and 259 ± 119 MP L^{-1} for MPs sized 125–150 μm and 425–500 μm, respectively. Statistically significant differences for MP per litre in surface runoff were not observed between the size fractions in either dry or wet runs (F (1, 236) = 0.13, $p = 0.72$). However, there was a statistically significant difference in MPs delivered per litre between the dry and wet runs with wet runs delivering fewer MPs (F (1, 236) = 247.12, $p < 0.001$). Overall, MPs transported in the surface runoff represented 18.8 ± 0.5% (25 431 ± 644 MPs) for the 125–150 μm MPs and 20.0 ± 0.1% (24 847 ± 150 MPs) for the 425–500 μm MPs of the total number of particles initially inputted into the plots ($n = 5$). No significant differences were observed in the overall number of MPs transport from the plots between size fractions (F (1, 216) = 0.18, $p = 0.68$).

Mean enrichment ratios (ER) for MPs after both the dry and wet runs showed strong evidence of enriched lateral transport of the 125–150 μm and 425–500 μm, with ER values of 5.8 ± 3.9 and 6.2 ± 4.5, respectively (Fig. 5). No significant difference was observed in the enrichment ratios between the two MP sizes across both dry and wet runs (χ^2 (1) = 0.22, $p = 0.64$). Overall, enrichment ratios for the dry runs were 8.6 ± 3.6 and 9.3 ± 4.6 for 125–150 μm and 425–500 μm MPs, respectively, whilst for wet runs these ratios were and 3.1 ± 1.8 and 3.2 ± 1.4 for 125–150 μm and 425–500 μm MPs, respectively. Wet runs had

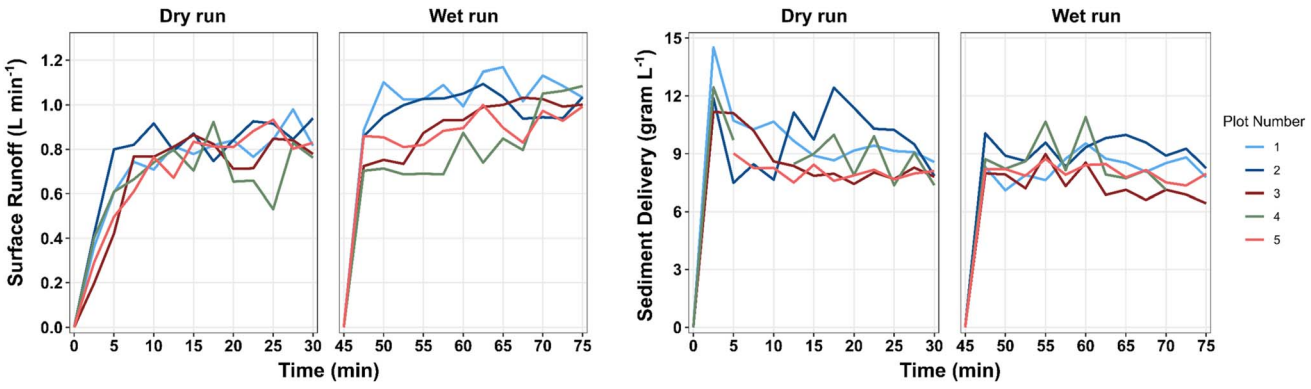

Fig. 3 Surface runoff and sediment flux during the rainfall simulations across the five plots ($n = 5$). Time 0 indicates the commencement of surface runoff. Missing data points in plot 4 are visible, these values were outliers and were excluded from the analysis.

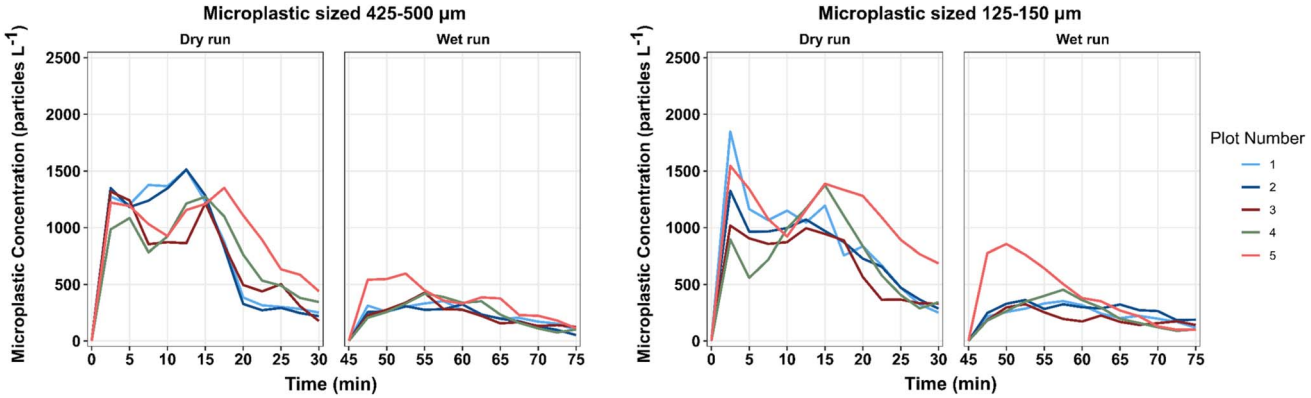

Fig. 4 MP particle sizes 425–500 µm and 125–150 µm transported in surface runoff across the five plots (n = 5). Time 0 indicates the commencement of surface runoff. The x-axis shows the time scale of the rainfall simulation (0–30 min dry run, 15 min of break, and 45–75 min wet run).

significantly lower enrichment ratios 3.2 ± 1.6 than the dry runs 9.0 ± 4.1 for both MP sizes (χ^2 (1) = 117.83, p < 0.001).

3.2 Patterns of microplastic movement on the surface of the soil

Images taken of the soil surface revealed the number of MPs present on the surface throughout the rainfall simulations. Across all plots, there were approximately 64% fewer 125–150 µm MPs (2819 ± 738) detected on the soil surface compared to the 425–500 µm MPs (7834 ± 540) before the start of the rainfall simulations. Fig. 6 reports changes in the number of particles detected on the soil surface during the rainfall simulations, expressed as a percentage of the number of particles detected prior to the start of the rainfall simulations.

During the dry runs, the 425–500 µm MPs showed a steady decline in particle number on the soil surface at the beginning of the simulation, followed by a period of relative stability, whereas the 125–150 µm MPs were associated with a sharper rate of disappearance from the soil surface at the beginning of the simulation, followed by a period of relative stability. There was a 95.9 ± 1.8% and 79.6 ± 1.6% reduction in the 125–150 µm and 425–500 µm MPs, respectively, from the soil surface over the course of the dry run simulation (Fig. 6). In the wet runs, there was a 13 ± 9.7% increase in the 425–500 µm MPs detected at the soil surface, and a 6.2 ± 5.3% decrease in the 125–150 µm MPs detected at the soil surface (Fig. 6). Overall, there was no significant difference in the percentage change between particle sizes (χ^2 (1) = 0.89, p = 0.34), but a significant difference was observed between the dry and wet conditions (χ^2 (1) = 11.29, p =

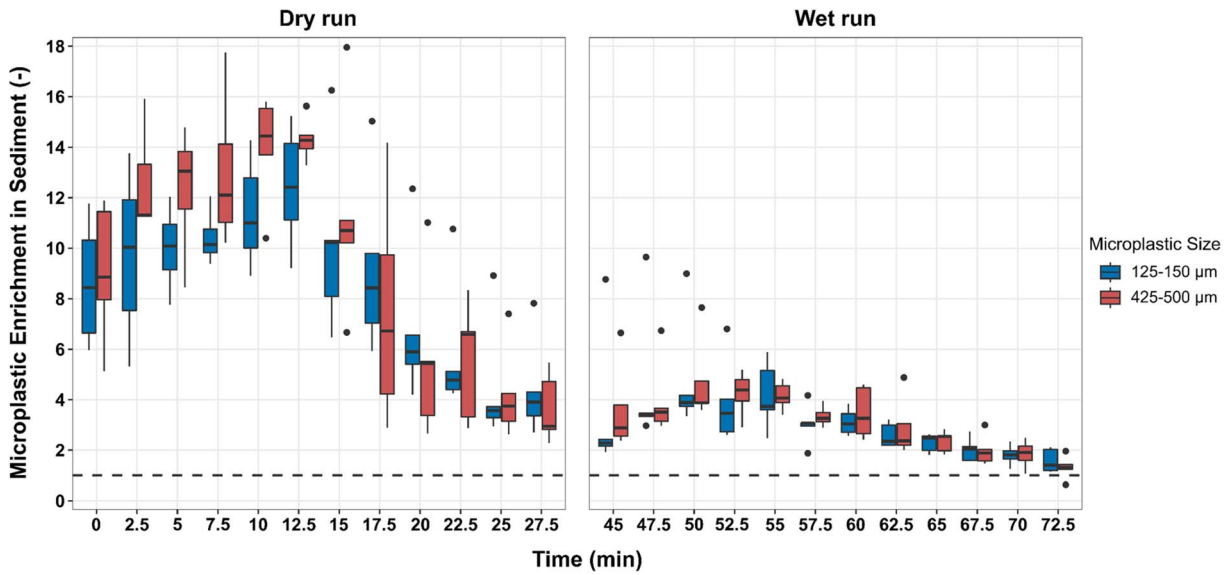

Fig. 5 Enrichment ratio of 125–150 µm and 425–500 µm MP in delivered sediments across rainfall simulations on all five plots for dry and wet runs (n = 5). Boxes show the medians, 1st and 3rd quartiles, whiskers represent the minimum and maximum values and dots represent outliers. A mean enrichment factor greater than 1 in all simulations indicates enriched transport of MP. The dashed line marks the initial concentration in the topsoil (<1 cm) as a factor 1.

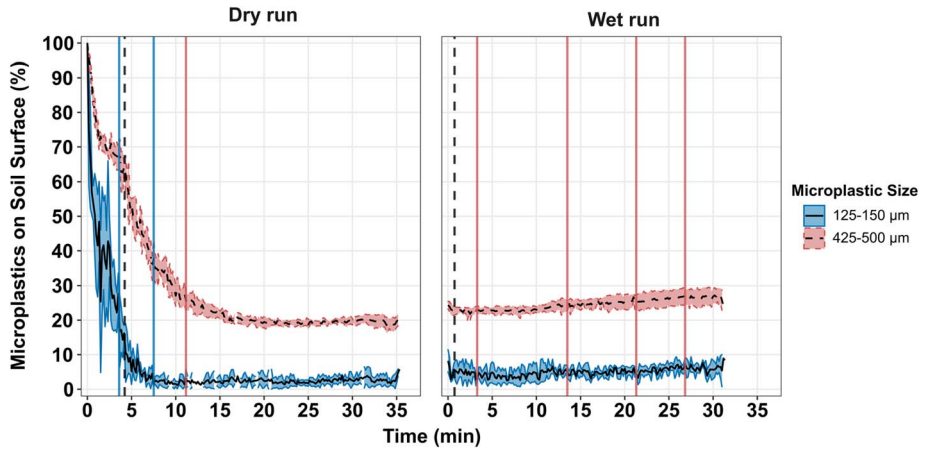

Fig. 6 Microplastics visible on the surface of the plots throughout the duration of rainfall simulations ($n = 4$). MP concentration is shown as percentage of particles with respect to the initial number of MPs detected on the soil surface for each plot and particle size. Black lines represent the mean particle number from all the plots and the shaded areas represent one standard deviation from the mean for each MP size. Red vertical lines indicate changepoints for the 425–500 µm MP, blue vertical lines indicate changepoints for the 125–150 µm MP and black dashed lines indicate the mean time for surface runoff commencement.

0.0008). As the mean time for the commencement of runoff from the plots was 4 min and 13 s ± 55 s during the dry run, the disappearance of particles in the first 4 min of the dry run rainfall simulation cannot be solely attributed to particles being transported from the plot *via* surface runoff.

A changepoint analysis of mean and variance was conducted to identify points at which the mean rate and variation of the rate of change in the number of particles detected on the soil surface shifted significantly. During the dry runs, 125–150 µm particles had a changepoint near that of runoff commencement, at 3 min and 40 s, as well as a changepoint later in the simulation at 7 min and 30 s. The 425–500 µm MPs had one significant changepoint in the dry runs 11 min and 10 s after the start of the rainfall simulation. This confirms that the number of 425–500 µm particles on the surface steadily declined throughout the simulation, and that surface runoff commencement did not increase the disappearance of these sized MPs from the soil surface significantly. In contrast, the 125–150 µm MPs detected at the soil surface showed multiple changepoints throughout the dry run simulations, indicating more variable rates of decline at the soil surface. In the wet run simulations, changepoints were identified at 3 min and 20 s, 13 min and 30 s, 21 min and 20 s, and 26 min and 50 s for the 425–500 µm MPs, showing the variable rates of increase of particles in this size range at the soil surface. No changepoints were detected for the 125–150 µm MPs in the wet runs, indicating a lack of significant changes in the number of these sized particles detected on the soil surface.

In the dry run prior to surface runoff, there was a 39 ± 10% (3100 ± 913 MPs) decrease in 425–500 µm MPs and 91 ± 4% (2573 ± 734 MPs) decrease in the 125–150 µm MPs detected on the soil surface (SI Fig. S2). After runoff commenced, there was a further 40 ± 9% (2724 ± 489 MPs) and 5 ± 4% (254 ± 172 MPs) decrease in MPs on the soil for the 425–500 µm MPs and 125–150 µm MP, respectively.

3.3 Vertical tracer movement and retention profile of microplastics

As the mass of collected soil samples varied, the concentration of MPs of different size ranges was normalized into particle number per kg of soil (Fig. 7). Most of the MPs remained in the 0–2 cm layer, with fewer particles found as depth increased. No MPs were detected in the soil below 8 cm depth. Overall, larger numbers of 425–500 µm MPs were detected in every soil layer as compared to either the 125–150 µm or 53–63 µm MPs, including in the 6–8 cm soil layer (Fig. 7).

Infiltration of the deuterium, (δ^2H), labelled water was visible in the upper soil depth (0–6 cm), whereas the contribution of labelled water diminished in the deeper soil layers (8–13

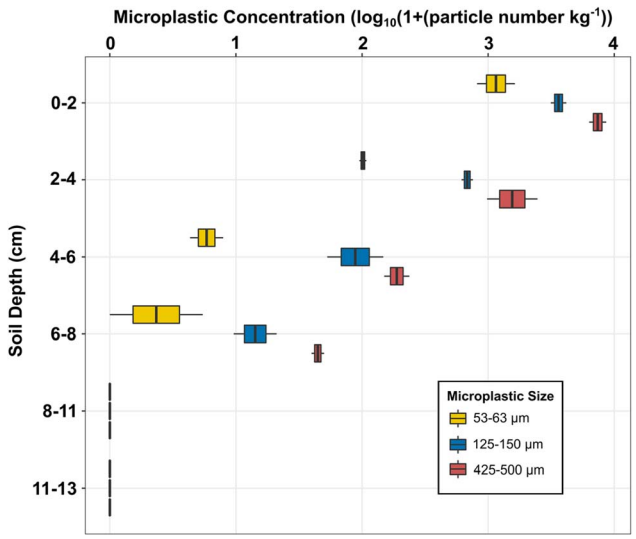

Fig. 7 The number of detected MPs by the mass of soil. Boxes show the medians, 1st and 3rd quartiles, whiskers represent the minimum and maximum values ($n = 2$).

cm) (SI Fig. S3b), indicating that the infiltrating water reached up to 8 cm depth after one hour of simulated rainfall. Further information regarding δ^2H can be found in SI 1.1.

Estimates of the number of MPs transported from the plots in surface runoff along with the number of MPs retained in the soil were summed and compared to the number of MPs initially inputted into the plots (1.35×10^5 for 125–150 μm MPs and 1.24×10^5 for 425–500 μm MPs) (SI Fig. S4). The number of MPs found in the soil samples at all depths were extrapolated to the area of the soil plot. Resulting in an estimated 61.3 ± 3.9% of MPs sized 125–150 μm and 139.8 ± 29.9% of MPs sized 425–500 μm were retained in the soil at the conclusion of the rainfall simulation. As reported above, 18.8 ± 0.5% of MPs sized 125–150 μm and 20.0 ± 0.1% (24 847 ± 150 MPs) of MPs sized 425–500 μm MPs were transported in surface runoff. Overall, MPs sized 125–150 μm and 425–500 μm had a recovery of approximately 80% and 160%, respectively.

4. Discussion

4.1 Pathways and rates of microplastic transport

In the dry runs prior to surface runoff, there were substantial decreases in particle numbers detected on the soil surface, reaching 39% for 425–500 μm MPs and 91% for the 125–150 μm MPs of the particle numbers prior to the start of the rainfall simulations. While it is possible that MPs were transported out of the plots through splash erosion processes,[48] visual inspection of the area surrounding the plot indicated a very small proportion of MPs were lost from the plots through this transport mechanism. Therefore, we assume that the substantial reduction in MPs detected at the soil surface during the rainfall simulations was due to MPs being incorporated into the soil matrix by raindrops mixing the near-surface layer of the soil.[48] Once mixed with the soil, MPs could be transported vertically into the soil profile by the infiltrating water.[25,26,59]

In this experiment, most MPs remained in the 0–2 cm soil layers, with decreasing numbers of MPs found as soil depth increased. Following a similar pattern to δ^2H, MPs of all size ranges were identified in soil layers as deep as 8 cm after 1 hour of rainfall simulation, indicating infiltrating water as the vector for MP transport vertically into the soil profile. However, no MPs were identified in the 8–13 cm layers of the soil as no substantial new rainwater went below this depth. Previous research has found similar patterns in which the majority of MPs inputted into a soil remains in the top few centimetres of soil, with decreasing numbers of MPs in the deeper soil layers after rainfall simulations.[27,60] One study found that over the course of 2 years MPs exposed to natural rainfall had minimal vertical transport and only migrated 8 cm.[61] This reduced vertical movement with infiltrating water could be due to a number of factors such as MPs blocking soil pores,[28] MP interactions with soil particles[8,34,35] and reduced pore space in tilled and repacked soils.[62] In addition to infiltrating water, MP vertical transport is aided by other processes such as soil biota[63,64] and tillage.[16,33] Heinze *et al.*[33] observed that over the course of 20 years MPs are quite mobile in the soil reaching depths of 70 cm, though most MPs remained in the top 20 cm plough layer of the soil.

The "first flush" phenomenon refers to the initial period of surface runoff when a pollutant is transported in higher concentrations than the latter stages of surface runoff.[65,66] This common trend was observed in our experiment where MPs in surface runoff for both wet and dry runs, were transported in higher numbers in the initial stages of surface runoff compared to the latter stages (Fig. 4). A side-by-side comparison of MPs and mineral soil particles showed that this initial flush of particles from soils is more pronounced for MP particles than for erodible mineral soil particles.[48] Enrichment ratios of MP delivery indicate that MP were transported more efficiently compared to sediments for both MPs sized 125–150 μm and 425–500 μm. Mean enrichment ratios of 9.3 for the 425–500 μm and 8.6 for the 125–150 μm were recorded during the dry runs, while the wet runs showed smaller enrichment ratios of 3.2 for the 425–500 μm and 3.1 for the 125–150 μm. In loamy sand soil, Rehm *et al.*[8] reported similar enrichment ratios of 8–11 for MPs (sized 250–300 μm and 53–100 μm) during an initial dry-run rainfall simulation, and 3–4 during the subsequent wet run. We did not observe significant differences in enrichment ratios between the large and small MP fraction as was shown in Rehm *et al.*[8] This probably resulted from different experimental set-ups, especially the short time between MP spiking and rainfall simulations which did not allow for aggregation between MP and mineral particles as was found for the small particles, in case of Rehm *et al.*[8] Overall, the enrichment ratios fluctuated through time mirroring the fluxes of MPs throughout the simulation. One explanation of the observed fluctuations in both MPs transported in surface runoff and the enrichment ratios is MPs vertical transport into the soil during the rainfall simulation by infiltration which may have removed MPs from the erodible layer.

Approximately, 19% and 20% of MP sized 125–150 μm and 425–500 μm, respectively, were transported in the surface runoff. Substantially more MPs sized 425–500 μm were detected in the soil samples compared to MPs sized 53–63 μm and 125–150 μm, which we attribute largely to the greater presence of 425–500 μm MPs at the sampling locations, rather than a systematic difference in detection efficiency across size ranges in the soil samples. Consequently, estimations of MPs remaining in the soil resulted in large discrepancies in the number balance (SI Fig. S4). However, as previously stated, visual inspection of the surrounding area suggested that MP transport outside the plots was minimal. Therefore, we assume that approximately 80% of the particles in this experiment were retained in the soil.

4.2 The relationship between microplastic size and transport

Much ambiguity surrounds MP transport processes as MPs themselves represent a diverse and everchanging range of polymer types of varying shape, sizes and levels of degradation.[67] Some attention has been given to the influence of size in determining the probability and rate of MP transport into the soil profile and over the soil surface.[8,25,27,38] In this study, we hypothesized that size would play an integral role in

determining the transport pathways as well as the number of MPs transported during the rainfall simulation. We hypothesized that the largest size fraction 425–500 μm would be primarily transported in the surface runoff in higher numbers compared to the other size fractions and MPs sized 125–150 μm infiltrate to greatest depth into the soil profile compared to the other size fractions.

While in our research, there was no significant difference in the number of MPs sized 125–150 μm and 425–500 μm transported from the plots *via* surface runoff, a slightly larger proportion of MPs sized 425–500 μm (20.0 ± 0.1%) were transported from the plots compared to MPs sized 125–150 μm (18.8 ± 0.5%). Similarly, Rehm *et al.*[8] found no significant difference in the number of MPs sized 53–100 μm and 250–300 μm transported from field plots *via* surface runoff. However, the authors also reported a slightly higher number of the largest size MP (250–300 μm) transported in surface runoff. Han *et al.*[38] found more plastics sized 250 μm transported from soil through surface runoff than plastics sized 1 mm, 4 mm, 15 mm and 50 mm, with no plastics >4 mm delivered in surface runoff. Zhang *et al.*,[27] found MPs sized <0.3 mm were transported in greater numbers than MPs sized 0.3–1 mm and 1–5 mm, though the number of MPs sized <0.3 mm were only transported in slightly higher number than MPs sized 0.3–1 mm. Liu *et al.*[37] found MPs <50 μm were transported in higher numbers than MPs sized 50–100 μm, 100–200 μm and 200–500 μm in surface runoff processes. Whilst research to date reports mixed influence of particle size on MP transport in surface runoff, it seems clear that MPs <1 mm are more likely to be transported than MPs >1 mm in surface runoff.

The transport of MPs vertically through the soil profile as influenced by MP size is better constrained in comparison to transport over the soil surface *via* surface runoff, although many studies have been conducted in columns with soil, sediment or glass beads which have a homogeneous size and shape. These studies report clear trends of deeper vertical movement for MPs of decreasing size.[28,29,59,68] There is less research investigating the vertical movement of MPs in complex field soils. In our research, we found clear evidence that MPs across size ranges 53–63 μm, 125–150 μm and 425–500 μm were transported as deep as water infiltrated into the soil profile (8 cm). As there were large discrepancies in the recovery between MP sizes (SI Fig. S4) we cannot claim that one size range was more mobile vertically compared to the other. Rather we affirm that larger MPs were found as deep in the soil compared to the smallest MP size investigated in this research. Research conducted by Du *et al.*[25] compared the vertical migration ability of MPs in three size ranges and found that 25–147 μm were the most mobile followed by 0–25 μm and then 147–250 μm MPs. Rehm *et al.*[8] in an 1.5 years experiment found a similar pattern were 53–100 μm MPs were more mobile vertically in the soil as compared to 250–300 μm MPs, though due to a relatively long experimental period other factors besides infiltrating water such as soil biota likely influenced MP vertical movement. Another study found MPs <0.3 mm were the most mobile vertically in the soil followed by MPs 0.3–1 mm with MPs 1–5 mm being the least mobile.[27] Results from our research and these studies indicate that the transport of MPs vertically in the soil does not necessarily follow a pattern, which is often seen in column experiments where, as MP size decreases the depth MPs are transported increases.

Altogether, current research suggests that both horizontal and vertical movement of MPs in the soil as influenced by size does not follow an inverse, linear relationship between MP size and mobility.[35] However, currently not enough empirical evidence exists to postulate the exact size ranges at which the probability of MP transport increases or decreases. Future work should be done on MPs of more size ranges to understand at which sizes the probability of MP transport increases or decreases under field conditions.

4.3 Broader environmental implication of microplastics transport from agricultural soils

While the findings from our research provides valuable insight into the transport processes of MPs in agricultural soil. We acknowledge that our experiment does not represent all environmental conditions and MP particles. First, MPs used in this experiment were spherical in shape, which are not commonly detected in agricultural soils. Microplastics are commonly found as fragments, films, fibers and particles, due to a broad range of input sources and degradation processes such as environmental weathering and mechanical abrasion.[69–71] The spherical shapes may have led to accelerated transport compared to MPs with irregular shapes,[72] though the MPs used in our study provided realistic density and size.[73–75] Additionally, MPs used in this study were pristine and thus represent the transport of MPs newly introduced into soils or rapidly mechanically fragmented.[16] Secondly, MP vertical and lateral transport rates and distances has been shown to vary dependent on soil texture,[8] rainfall intensity,[27,37,38] and soil slope[27,76] and thus our experiment represent only a subset of possible environmental scenarios.

However, this research builds on knowledge gained from laboratory experiments to provide a more realistic understanding of vertical and lateral transport processes. This research presents, for the first time, an analysis of MP transport pathways and relative proportions MPs of various size are transported during a heavy rainfall event under field conditions. We found that the majority of MPs were retained in the soil and MPs of all sizes were detected as deep as 8 cm. A fair portion (20%) of MPs were transported in surface runoff and were enriched in sediments demonstrating MPs are more mobile than mineral soil particles.

These findings add empirical evidence to the widely held view that soils possess a high capacity to retain MPs and can act as long-term sinks.[77] Schell *et al.*[60] found a high retention rate of MPs in soils amended with sewage sludge with less than 1% of MPs transported in surface runoff over the period of 1 year. The higher rates of MPs transported in our research is likely due to the highly organic sewage sludge in their experiment aiding in the retention of MPs[78,79] and the higher rainfall intensity applied to our soil. Despite their retention in soil, our research demonstrated that MPs are more easily transported than soil

particles, indicating that erodible, MP contaminated soils may serve as significant sources to surrounding environments.[7,9]

Given the widespread use of plastic materials in agriculture and the persistence of many conventional MPs in the environment, the results of this study underscore the need for improved management practices to mitigate the accumulation of MPs in soil systems and the export of MPs from terrestrial into aquatic ecosystems. While soil conservation practices reduce the lateral transport of MPs, for example increasing vegetation density, these effects have been shown to be dependent on polymer size and shape.[38,80] Regarding the vertical movement of MPs, previous research demonstrates that soil management practices and MP incorporation into aggregates may limit MP transport vertically through the soil profile.[8,33] Further empirical research should be conducted to test the effectiveness of these and other strategies to reduce MP transport both vertically into the soil and laterally over the soil surface.

5. Conclusion

Microplastics (MPs) are a contaminant of emerging concern, transported through diverse ecosystems across the globe. In this research, we investigated the transport of MPs of various sizes from agricultural soil during erosion processes induced through rainfall. The results from this research show that MPs are simultaneously transported both vertically into the soil profile with infiltrating water and laterally in surface runoff during heavy rainfall events. Though, the majority of MPs were retained in the soil, indicating that soils should be considered sinks, the proportion of MPs which were transported in surface runoff was not trivial demonstrating soils are sources for MP pollution. MPs sized 125–150 μm and 425–500 μm exhibited distinct patterns of movement from the surface of the soil but ultimately were transported in surface runoff in nearly equal numbers. This result provides insufficient evidence to support our first hypothesis that MPs sized 425–500 μm would be transported in higher numbers in surface runoff compared to MPs sized 125–150 μm. MPs of each size range 53–63 μm, 125–150 μm, and 425–500 μm were each detected in the soil as deep as 8 cm, providing insufficient evidence to support our second hypothesis that there would be a size-dependent vertical transportation. This challenges the current assumption that as MP size decreases the likelihood of MP mobility increases, underscoring the complexity of MP transport dynamics in soils. While further research is needed not only to deepen our understanding of how MPs are transported within and from soils, steps should be taken to reduce the amount of MPs entering into agricultural soils in order to limit global MP pollution.

Conflicts of interest

The authors declare no conflicts of interest.

Data availability

Data is available *via* Zenodo: **https://doi.org/10.5281/zenodo.14468499**.

Supplementary information is available. The SI provides text and figures describing: the analysis of deuterium in the water and soil water (Text S1) and image analysis scripts (Text S2), microscope image of MP used in the experiment (Fig. S1), the percentage of MP detected on the soil surface before and after surface runoff (Fig. S2), deuterium content of simulated rainwater and soil (Fig. S3), mass balance of MPs (Fig. S4). See DOI: **https://doi.org/10.1039/d5em00304k**.

Acknowledgements

This project has received funding from the European Union's Horizon 2020 research and innovation programme under the Marie Skłodowska-Curie grant agreement no. 955334. The authors would like to express their sincere appreciation to Martin Neumann, and Tomas Laburda at CVUT for their technical support as well as Mengyi Gong for her advice on time series statistical analysis.

References

1 S. Samandra, J. M. Johnston, J. E. Jaeger, B. Symons, S. Xie, M. Currell, A. V. Ellis and B. O. Clarke, Microplastic contamination of an unconfined groundwater aquifer in Victoria, Australia, *Sci. Total Environ.*, 2022, **802**, 149727.
2 S.-A. Strungaru, R. Jijie, M. Nicoara, G. Plavan and C. Faggio, Micro- (nano) plastics in freshwater ecosystems: Abundance, toxicological impact and quantification methodology, *Trac. Trends Anal. Chem.*, 2019, **110**, 116–128.
3 O. R. Umeh, D. U. Ophori, E. M. Ibo, C. I. Eke and T. P. Oyen, Groundwater systems under siege: The silent invasion of microplastics and cock-tails worldwide, *Environ. Pollut.*, 2024, **356**, 124305.
4 C. Scherer, R. Wolf, J. Völker, F. Stock, N. Brennhold, G. Reifferscheid and M. Wagner, Toxicity of microplastics and natural particles in the freshwater dipteran Chironomus riparius: Same same but different?, *Sci. Total Environ.*, 2020, **711**, 134604.
5 O. A. Vázquez and M. S. Rahman, An ecotoxicological approach to microplastics on terrestrial and aquatic organisms: A systematic review in assessment, monitoring and biological impact, *Environ. Toxicol. Pharmacol.*, 2021, **84**, 103615.
6 S. Ziajahromi, A. Kumar, P. A. Neale and F. D. L. Leusch, Environmentally relevant concentrations of polyethylene microplastics negatively impact the survival, growth and emergence of sediment-dwelling invertebrates, *Environ. Pollut.*, 2018, **236**, 425–431.
7 M. Norling, R. Hurley, T. Schell, M. N. Futter, A. Rico, M. Vighi, A. Blanco, J. L. J. Ledesma and L. Nizzetto, Retention efficiency for microplastic in a landscape estimated from empirically validated dynamic model predictions, *J. Hazard. Mater.*, 2024, **464**, 132993.

8 R. Rehm, T. Zeyer, A. Schmidt and P. Fiener, Soil erosion as transport pathway of microplastic from agriculture soils to aquatic ecosystems, *Sci. Total Environ.*, 2021, 148774.
9 R. Rehm and P. Fiener, Model-based analysis of erosion-induced microplastic delivery from arable land to the stream network of a mesoscale catchment, *Soil*, 2024, **10**, 211–230.
10 L. Su, X. Xiong, Y. Zhang, C. Wu, X. Xu, C. Sun and H. Shi, Global transportation of plastics and microplastics: A critical review of pathways and influences, *Sci. Total Environ.*, 2022, **831**, 154884.
11 J. Wang, K. Bucci, P. A. Helm, T. Hoellein, M. J. Hoffman, R. Rooney and C. M. Rochman, Runoff and discharge pathways of microplastics into freshwater ecosystems: A systematic review and meta-analysis, *FACETS*, 2022, **7**, 1473–1492.
12 R. Pereira, A. Hernandez, B. James, B. LeMoine, C. Carranca, F. Rayns, G. Cornelis, L. Erälinna, L. Czech and P. Picuno, *EIP-AGRI Focus Group Reducing the Plastic Footprint of Agriculture FINAL REPORT*, European Commission, 2021.
13 S. J. Cusworth, W. J. Davies, M. R. McAinsh and C. J. Stevens, Sustainable production of healthy, affordable food in the UK: The pros and cons of plasticulture, *Food Energy Secur.*, 2022, e404.
14 FAO, *Assessment of Agricultural Plastics and Their Sustainability: A Call for Action*, Rome, Italy, 2021.
15 P. Feuilloley, G. Cesar, L. Benguigui, Y. Grohens, I. Pillin, H. Bewa, S. Lefaux and M. Jamal, Degradation of polyethylene designed for agricultural purposes, *J. Polym. Environ.*, 2005, **13**, 349–355.
16 A. Maqbool, G. Guzmán, P. Fiener, F. Wilken, M.-A. Soriano and J. A. Gómez, Tracing macroplastics redistribution and fragmentation by tillage translocation, *J. Hazard. Mater.*, 2024, **477**, 135318.
17 F. Corradini, P. Meza, R. Eguiluz, F. Casado, E. Huerta-Lwanga and V. Geissen, Evidence of microplastic accumulation in agricultural soils from sewage sludge disposal, *Sci. Total Environ.*, 2019, **671**, 411–420.
18 K. A. V. Zubris and B. K. Richards, Synthetic fibers as an indicator of land application of sludge, *Environ. Pollut.*, 2005, **138**, 201–211.
19 M. Braun, M. Mail, A. E. Krupp and W. Amelung, Microplastic contamination of soil: Are input pathways by compost overridden by littering?, *Sci. Total Environ.*, 2023, **855**, 158889.
20 N. Weithmann, J. N. Möller, M. G. Löder, S. Piehl, C. Laforsch and R. Freitag, Organic fertilizer as a vehicle for the entry of microplastic into the environment, *Sci. Adv.*, 2018, **4**, eaap8060.
21 S. Peneva, Q. N. Phan Le, D. R. Munhoz, O. Wrigley, G. P. F. Macan, H. Doose, W. Amelung and M. Braun, Plastic input and dynamics in industrial composting, *Waste Manag.*, 2025, **193**, 283–292.
22 F. Sommer, V. Dietze, A. Baum, J. Sauer, S. Gilge, C. Maschowski and R. Gieré, Tire abrasion as a major source of microplastics in the environment, *Aerosol Air Qual. Res.*, 2018, **18**, 2014–2028.
23 J. Brahney, M. Hallerud, E. Heim, M. Hahnenberger and S. Sukumaran, Plastic rain in protected areas of the United States, *Science*, 2020, **368**, 1257–1260.
24 A. Chamas, H. Moon, J. Zheng, Y. Qiu, T. Tabassum, J. H. Jang, M. Abu-Omar, S. L. Scott and S. Suh, Degradation Rates of Plastics in the Environment, *ACS Sustain. Chem. Eng.*, 2020, **8**, 3494–3511.
25 A. Du, C. Hu, X. Wang, Y. Zhao, W. Xia, X. Dai, L. Wang and S. Zhang, Experimental Study on the Migration and Distribution of Microplastics in Desert Farmland Soil Under Drip Irrigation, *Environ. Toxicol. Chem.*, 2024, **43**, 1250–1259.
26 A. Maqbool, W. Li, C. Stumpp, M.-A. Soriano and J. A. Gómez, Effect of Preferential Microplastics Leaching Through Macropores on Vertical Soil Particle Transport, *Eur. J. Soil Sci.*, 2025, **76**, e70140.
27 X. Zhang, Y. Chen, X. Li, Y. Zhang, W. Gao, J. Jiang, A. Mo and D. He, Size/shape-dependent migration of microplastics in agricultural soil under simulative and natural rainfall, *Sci. Total Environ.*, 2022, **815**, 152507.
28 W. Li, G. Brunetti, C. Zafiu, M. Kunaschk, M. Debreczeby and C. Stumpp, Experimental and simulated microplastics transport in saturated natural sediments: Impact of grain size and particle size, *J. Hazard. Mater.*, 2024, **468**, 133772.
29 V. P. Ranjan, A. Joseph, H. B. Sharma and S. Goel, Preliminary investigation on effects of size, polymer type, and surface behaviour on the vertical mobility of microplastics in a porous media, *Sci. Total Environ.*, 2023, **864**, 161148.
30 K. Waldschläger and H. Schüttrumpf, Infiltration Behavior of Microplastic Particles with Different Densities, Sizes, and Shapes—From Glass Spheres to Natural Sediments, *Environ. Sci. Technol.*, 2020, **54**, 9366–9373.
31 C. Rieckhof, V. Martínez-Hernández, E. Holzbecher and R. Meffe, Effect of particle size on the transport of polystyrene micro- and nanoplastic particles through quartz sand under unsaturated conditions, *Environ. Pollut.*, 2024, **363**, 125193.
32 L. Heerey, J. J. O'Sullivan, M. Bruen, J. Turner, A. M. Mahon, S. Murphy, H. T. Lally, J. D. O'Connor, I. O'Connor and R. Nash, Export pathways of biosolid derived microplastics in soil systems – Findings from a temperate maritime climate, *Sci. Total Environ.*, 2023, **888**, 164028.
33 W. M. Heinze, Z. Steinmetz, N. D. R. Klemmensen, J. Vollertsen and G. Cornelis, Vertical distribution of microplastics in an agricultural soil after long-term treatment with sewage sludge and mineral fertiliser, *Environ. Pollut.*, 2024, **356**, 124343.
34 B. Chang, B. He, G. Cao, Z. Zhou, X. Liu, Y. Yang, C. Xu, F. Hu, J. Lv and W. Du, Co-transport of polystyrene microplastics and kaolinite colloids in goethite-coated quartz sand: Joint effects of heteropolymerization and surface charge modification, *Sci. Total Environ.*, 2023, **884**, 163832.
35 H. Luo, L. Chang, T. Ju and Y. Li, Factors Influencing the Vertical Migration of Microplastics up and down the Soil Profile, *ACS Omega*, 2024, **9**, 50064–50077.

36 Y. T. He, J. Wan and T. Tokunaga, Kinetic stability of hematite nanoparticles: the effect of particle sizes, *J. Nanoparticle Res.*, 2008, **10**, 321–332.
37 D. Liu, Z. Yang, Y. Gong, D. Song and Y. Chen, Occurrence and emission characteristics of microplastics in agricultural surface runoff under different natural rainfall and short-term fertilizer application, *J. Hazard. Mater.*, 2024, **477**, 135254.
38 N. Han, Q. Zhao, H. Ao, H. Hu and C. Wu, Horizontal transport of macro- and microplastics on soil surface by rainfall induced surface runoff as affected by vegetations, *Sci. Total Environ.*, 2022, **831**, 154989.
39 K. Waldschläger and H. Schüttrumpf, Erosion Behavior of Different Microplastic Particles in Comparison to Natural Sediments, *Environ. Sci. Technol.*, 2019, **53**, 13219–13227.
40 J. Jeřábek, D. Zumr, T. Laburda, J. Krása and T. Dostál, Soil surface connectivity of tilled soil with wheel tracks and its development under simulated rainfall, *J. Hydrol.*, 2022, **613**, 128322.
41 T. Li, J. Jeřábek, J. Winkler, M. D. Vaverková and D. Zumr, Effects of prescribed fire on topsoil properties: a small-scale straw burning experiment, *J. Hydrol. Hydromech.*, 2022, **70**, 450–461.
42 J. Stašek, J. Krása, M. Mistr, T. Dostál, J. Devátý, T. Středa and J. Mikulka, Using a Rainfall Simulator to Define the Effect of Soil Conservation Techniques on Soil Loss and Water Retention, *Land*, 2023, **12**, 431.
43 N. Zambon, L. L. Johannsen, P. Strauss, T. Dostal, D. Zumr, T. A. Cochrane and A. Klik, Splash erosion affected by initial soil moisture and surface conditions under simulated rainfall, *Catena*, 2021, **196**, 104827.
44 M. Uber, M. Haller, C. Brendel, G. Hillebrand and T. Hoffmann, Past, present and future rainfall erosivity in central Europe based on convection-permitting climate simulations, *Hydrol. Earth Syst. Sci.*, 2024, **28**, 87–102.
45 E. N. Mueller and A. Pfister, Increasing occurrence of high-intensity rainstorm events relevant for the generation of soil erosion in a temperate lowland region in Central Europe, *J. Hydrol.*, 2011, **411**, 266–278.
46 P. Kavka and M. Neumann, Swinging-pulse sprinkling head for rain simulators, *Hydrology*, 2021, **8**, 74.
47 M. Neumann, P. Kavka, J. Devátý, J. Stašek, L. Strouhal, A. Tejkl, R. Kubínová and J. Rodrigo-Comino, Effect of plot size and precipitation magnitudes on the activation of soil erosion processes using simulated rainfall experiments in vineyards, *Front. Environ. Sci.*, 2022, **10**, 949774.
48 E. Severe, B. W. J. Surridge, P. Fiener, M. P. Coogan, R. H. Platel, M. R. James and J. Quinton, The Transport of Microplastics from Soil in Response to Surface Runoff and Splash Erosion, *Environ. Sci. Technol.*, 2025, **59**(27), 14063–14074.
49 C. M. Bowers and R. J. Johansen, Photographic evidence protocol: the use of digital imaging methods to rectify angular distortion and create life size reproductions of bite mark evidence, *J. Forensic Sci.*, 2002, **47**, 178–185.
50 K. S. Collins and M. F. Gazley, Does my posterior look big in this? The effect of photographic distortion on morphometric analyses, *Paleobiology*, 2017, **43**, 508–520.
51 C. Mutchler, C. Murphree and K. McGregor, in *Soil Erosion Research Methods*, Soil and Water Conservation Society Ankeny, IA., 1994, pp. 11–37.
52 D. W. Cromey, Avoiding Twisted Pixels: Ethical Guidelines for the Appropriate Use and Manipulation of Scientific Digital Images, *Sci. Eng. Ethics*, 2010, **16**, 639–667.
53 S. Sinha Ray, D. Zumr, F. Wilken, T. Dostál and P. Fiener, A cost-effective protocol for detecting fluorescent microplastics in arable soils to study redistribution processes, *Polym. Test.*, 2025, **147**, 108824.
54 M. M. Maw, N. Boontanon, S. Fujii and S. K. Boontanon, Rapid and efficient removal of organic matter from sewage sludge for extraction of microplastics, *Sci. Total Environ.*, 2022, **853**, 158642.
55 L. I. Wassenaar, M. J. Hendry, V. L. Chostner and G. P. Lis, High Resolution Pore Water δ2H and δ18O Measurements by H2O(liquid)−H2O(vapor) Equilibration Laser Spectroscopy, *Environ. Sci. Technol.*, 2008, **42**, 9262–9267.
56 L. Boumaiza, R. Chesnaux, T. Drias, R. L. Stotler, G. Skrzypek, M. Gillon, H. Wanke, K. H. Johannesson and C. Stumpp, Vadose zone water stable isotope profiles for assessing groundwater recharge:Sensitivityto seasonal soil sampling, *J. Hydrol.*, 2023, **626**, 130291.
57 *R Core Team*, 2023.
58 R. Killick and I. A. Eckley, changepoint: An R Package for Changepoint Analysis, *J. Stat. Softw.*, 2014, **58**, 1–19.
59 D. O'Connor, S. Pan, Z. Shen, Y. Song, Y. Jin, W.-M. Wu and D. Hou, Microplastics undergo accelerated vertical migration in sand soil due to small size and wet-dry cycles, *Environ. Pollut.*, 2019, **249**, 527–534.
60 T. Schell, R. Hurley, N. T. Buenaventura, P. V. Mauri, L. Nizzetto, A. Rico and M. Vighi, Fate of microplastics in agricultural soils amended with sewage sludge: Is surface water runoff a relevant environmental pathway?, *Environ. Pollut.*, 2022, **293**, 118520.
61 R. B. Schefer, J. Koestel and D. M. Mitrano, Minimal vertical transport of microplastics in soil over two years with little impact of plastics on soil macropore networks, *Commun. Earth Environ.*, 2025, **6**, 278.
62 L. F. Pires, J. A. R. Borges, J. A. Rosa, M. Cooper, R. J. Heck, S. Passoni and W. L. Roque, Soil structure changes induced by tillage systems, *Soil Tillage Res.*, 2017, **165**, 66–79.
63 W. M. Heinze, D. M. Mitrano, E. Lahive, J. Koestel and G. Cornelis, Nanoplastic Transport in Soil via Bioturbation by Lumbricus terrestris, *Environ. Sci. Technol.*, 2021, **55**, 16423–16433.
64 E. Huerta Lwanga, H. Gertsen, H. Gooren, P. Peters, T. Salánki, M. van der Ploeg, E. Besseling, A. A. Koelmans and V. Geissen, Incorporation of microplastics from litter into burrows of Lumbricus terrestris, *Environ. Pollut.*, 2017, **220**, 523–531.
65 S. Li, X. Wang, B. Qiao, J. Li and J. Tu, First flush characteristics of rainfall runoff from a paddy field in the

Taihu Lake watershed, China, *Environ. Sci. Pollut. Res.*, 2017, **24**, 8336–8351.
66 L. B. Faucette, L. M. Risse, M. A. Nearing, J. W. Gaskin and L. T. West, Runoff, erosion, and nutrient losses from compost and mulch blankets under simulated rainfall, *J. Soil Water Conserv.*, 2004, **59**, 154–160.
67 M. Kooi and A. A. Koelmans, Simplifying Microplastic via Continuous Probability Distributions for Size, Shape, and Density, *Environ. Sci. Technol. Lett.*, 2019, **6**, 551–557.
68 S. Qi, J. Song, J. Shentu, Q. Chen and K. Lin, Attachment and detachment of large microplastics in saturated porous media and its influencing factors, *Chemosphere*, 2022, **305**, 135322.
69 L. Cao, D. Wu, P. Liu, W. Hu, L. Xu, Y. Sun, Q. Wu, K. Tian, B. Huang, S. J. Yoon, B.-O. Kwon and J. S. Khim, Occurrence, distribution and affecting factors of microplastics in agricultural soils along the lower reaches of Yangtze River, China, *Sci. Total Environ.*, 2021, **794**, 148694.
70 M. O. Akca, S. Gündoğdu, H. Akca, R. A. Delialioğlu, C. Aksit, O. C. Turgay and N. Harada, An evaluation on microplastic accumulations in Turkish soils under different land uses, *Sci. Total Environ.*, 2024, **911**, 168609.
71 S. Piehl, A. Leibner, M. G. Löder, R. Dris, C. Bogner and C. Laforsch, Identification and quantification of macro-and microplastics on an agricultural farmland, *Sci. Rep.*, 2018, **8**, 1–9.
72 H. Yang, X. Lin, J. Lu, X. Zhao, D. Wu, H. Kim, L. Su and L. Cai, Effect of shape on the transport and retention of nanoplastics in saturated quartz sand, *J. Hazard. Mater.*, 2024, **479**, 135766.
73 J. Álvarez-Lopeztello, C. Robles and R. F. del Castillo, Microplastic pollution in neotropical rainforest, savanna, pine plantations, and pasture soils in lowland areas of Oaxaca, Mexico: Preliminary results, *Ecol. Indic.*, 2021, **121**, 107084.
74 M. Scheurer and M. Bigalke, Microplastics in Swiss Floodplain Soils, *Environ. Sci. Technol.*, 2018, **52**, 3591–3598.
75 G. S. Zhang and Y. F. Liu, The distribution of microplastics in soil aggregate fractions in southwestern China, *Sci. Total Environ.*, 2018, **642**, 12–20.
76 N. Han, Q. Zhao and C. Wu, Threshold migration conditions of (micro) plastics under the action of overland flow, *Water Res.*, 2023, **242**, 120253.
77 E. H. Lwanga, N. Beriot, F. Corradini, V. Silva, X. Yang, J. Baartman, M. Rezaei, L. van Schaik, M. Riksen and V. Geissen, Review of microplastic sources, transport pathways and correlations with other soil stressors: a journey from agricultural sites into the environment, *Chem. Biol. Technol. Agric.*, 2022, **9**, 20.
78 S. Wagner, S. R. Cattle and T. Scholten, Soil-aggregate formation as influenced by clay content and organic-matter amendment, *J. Plant Nutr. Soil Sci.*, 2007, **170**, 173–180.
79 Y. Liang, A. Lehmann, G. Yang, E. F. Leifheit and M. C. Rillig, Effects of Microplastic Fibers on Soil Aggregation and Enzyme Activities Are Organic Matter Dependent, *Front. Environ. Sci.*, 2021, **9**, 97.
80 N. A. Forster, S. C. Wilson and M. K. Tighe, Microplastic surface retention and mobility on hiking trails, *Environ. Sci. Pollut. Res.*, 2023, **30**, 46368–46382.